Estimating the distribution of RCS using sparse measured samples

Minna Väilä, Juha Jylhä, Marja Ruotsalainen, and Henna Perälä
Laboratory of Signal Processing
Tampere University of Technology
Tampere, Finland
Email: minna.vaila@tut.fi

***Abstract*—In this paper, we consider estimating the distribution of the radar cross section (RCS) using a small number of sparse measured samples. With a small sample size, it is advantageous to use the measured samples in combination with a preliminary description of the RCS, such as a distribution produced from simulated RCS samples. We estimate the RCS taking the target aspect angle into account and consider its uncertainty by representing each sample with a probability distribution over the aspect angle space instead of a single value. Thus, the aspect angle of a measured sample may be represented by an inexact estimate rather than an accurate value. In addition to the approach to estimating the RCS, we propose ways of analyzing the performance attained with it and apply them to a case study. Although the analysis performed with a single test object does not provide quantitative results, it offers a demonstration of the approach and a preliminary assessment of its performance.**

I. Introduction

The radar cross section (RCS) is a measure describing the electromagnetic scattering of an object. It is influenced by a number of factors termed the operating conditions, which relate to the properties of the object and the radar measurement. As a simplification to the complicated nature of the electromagnetic scattering phenomenon, the RCS of practical targets has usually been treated as a statistically characterized random variable [1], [2]. However, the statistical characteristics of RCS are known to vary with the aspect angle and are often represented inadequately with a single type of density function [3], [4].

In this paper, we consider estimating the distribution of RCS using a small number of sparse measured samples and assume the samples to have some uncertainty about the target aspect angle. The samples may be produced by a real-time system measuring non-cooperative targets or a more controlled measurement setup. In a real-time application, the sample size may be small and the samples often spread unevenly over the aspect angles. The objective is to estimate the RCS for any aspect angle using this sparse sample set. The accuracy of the estimation is naturally dependent on the representativeness of the sample set; with few samples, traditional methods relying on e.g. spline interpolation [5] produce a poor result. Thus, we hypothesize it is advantageous to use the sparse sample set in combination with a preliminary description of the RCS, such as a distribution produced from simulated RCS samples.

We have previously introduced the concepts for considering the uncertainty of the aspect angle in the context of non-cooperative target recognition (NCTR) [6]. Additionally, we have applied these principles to the estimation of a dynamic RCS distribution for a specific flight path of a target [7] and to radar performance prediction [8]. In this paper, we extend them to estimating the distribution of RCS using a small number of measured samples. The proposed approach aims to benefit NCTR and radar performance prediction. We demonstrate it through a case study to analyze its performance relating to these potential applications.

II. Estimating the RCS distribution using measured samples

In this section, we describe the method for estimating the distribution of RCS using sparse measured samples. We estimate the RCS taking the target aspect angle into account and consider two sources of uncertainty about the aspect angle: the uncertainty related to the application of the estimated RCS distribution and the uncertainty related to the samples used in the estimation. First, we describe the general form for the estimation of the RCS where we consider only the former source of uncertainty. In this case, we assume to know the exact aspect angles for the samples. Then, we include the latter source of uncertainty in the estimation to allow the use of samples, for which we do not know the exact aspect angle but can form a probabilistic description. Finally, we describe how the proposed concepts can be used in combination with a preliminary distribution of lower quality, which is based on e.g. simulated RCS.

A. Estimating the RCS distribution using samples with known aspect angles

In the following formulation, we assume to know the exact values of the aspect angles for the samples we use in the estimation of the distribution. This can be achieved by using RCS samples produced through e.g. a simulation or a controlled measurement on a turntable. As in our previous work, we use a histogram to estimate the aspect-angle-specific distribution of RCS and the probability of occurrence $p(\alpha_k, \alpha)$ to incorporate in the estimation the uncertainty about the target aspect angle α related to its application or context [7], [8]. The concept of $p(\alpha_k, \alpha)$ is reasonable only when we can assume there is uncertainty about α. It defines the probability of α_k being the true aspect angle when we estimate the distribution for the aspect angle α. In the context of NCTR, for instance, the precise value of the target aspect angle α is unknown but we may have an estimate for it. Then again, in the context of

radar performance prediction, the $p(\alpha_k, \alpha)$ is comparable to the result of a Monte Carlo simulation of a particular flight path for one time instant with α as the most probable aspect angle; we have discussed this topic in more detail in [7].

We compile the histogram using the RCS samples corresponding to the aspect angles α_k by weighting each sample $s_k \in S$ according to $p(\alpha_k, \alpha)$. The ith bin of the histogram $h(\alpha|S)$ corresponding to the aspect angle α is formulated as

$$h_i(\alpha|S) = \sum_{k=1}^{K} y_i(s_k) \cdot p(\alpha_k, \alpha) \quad (1)$$

where K is the number of RCS samples,

$$y_i(s) = \begin{cases} 1, & \text{if } s \in \Delta_i \\ 0, & \text{otherwise} \end{cases} \quad (2)$$

and Δ_i defines the ith histogram bin. Please note that the estimation of $h(\alpha|S)$ does not pose restrictions on the sampling of s_k, and allows α_k to spread sparsely around the aspect angle α. In this paper, we assume the probability of occurrence $p(\alpha_k, \alpha)$ symmetrical in regard to the azimuth and elevation component of the aspect angle, its sum over α_k normalized to one, and $p(\alpha_k, \alpha) \sim N(\alpha, \sigma_1^2)$. The standard deviation σ_1 corresponds to the amount of aspect angle uncertainty related to the application of $h(\alpha|S)$.

B. Estimating the RCS distribution using samples with uncertain aspect angles

Next, we modify the formulation of (1) to allow the use of samples, for which we do not know the exact aspect angle but can form a probabilistic description. This description is similar to the probability of occurrence $p(\alpha_k, \alpha)$ we introduced in Section II-A. Thus, we use the similar notation $p(\alpha_j, \alpha_k)$ for the samples $s_k \in S$. Here, α_k correspond to the estimated aspect angles for the measured samples s_k.

As in Section II-A, we assume that $p(\alpha_j, \alpha_k) \sim N(\alpha_k, \sigma_2^2)$. The standard deviation σ_2 corresponds to the amount of the aspect angle uncertainty of the RCS samples S used in the estimation. We define a set of aspect angles α_j as the sampling points of the probability distribution, i.e. the instances we compile in the histogram. We assume the sum of $p(\alpha_j, \alpha_k)$ over both α_j and α_k to be normalized to one in order to produce a normalized histogram. Assuming a set of RCS samples S, the ith bin of the aspect-angle-specific histogram $h(\alpha|S)$ can be formulated as

$$h_i(\alpha|S) = \sum_{j=1}^{J} \sum_{k=1}^{K} y_i(s_k) \cdot p(\alpha_j, \alpha_k) \cdot p(\alpha_j, \alpha), \quad (3)$$

where J is the number of sampling points we compile in the histogram, K the number of samples, and $y_i(s_k)$ corresponds to (2). The formulation of (3) actually represents a more general form of (1), where we assumed the aspect angle for each RCS sample compiled in the histogram to be known exactly. In (3) the same effect would be achieved using $p(\alpha_j, \alpha_k) \sim N(\alpha_k, \sigma_2^2)$ with $\sigma_2 = 0°$.

C. Refining a preliminary distribution using samples with uncertain aspect angles

If the number of RCS samples we have at our disposal is low, the estimation of the RCS produces an inadequate result, especially for the aspect angles represented poorly in the data. However, we can use these samples to refine a preliminary RCS distribution, estimated based on e.g. simulated RCS samples. A straight-forward way to accomplish this is to compile the aspect-angle-specific histograms separately from both data and combine them as a weighted sum. We define w_1 as the weight of the preliminary histogram based on more complete data and w_2 as the weight of the histogram based on the few sparse samples. To preserve the mass of the histogram, we further define both these weights to be positive and their sum equal to one. We can formulate w_1 as the complement of w_2

$$w_1 = 1 - w_2. \quad (4)$$

With this formulation, the histogram compiled using the sparse sample set S_2 is given an equal weight w_2 for all α, although only α with a reasonable number of samples around them produce a sensible result. In these cases, it is reasonable to increase the value of w_1 and reformulate (4) as a function of α.

$$w_1(\alpha|S_2) = \begin{cases} 0, & \text{if } w_2 = 1 \\ 1 - w_2 \sum_i h_i(\alpha|S_2), & \text{otherwise.} \end{cases} \quad (5)$$

This reformulation requires a redefinition of $p(\alpha_j, \alpha_k)$ as well: it needs to be normalized only over α_j, giving each measured sample the overall contribution of one, but limited to a certain value over α_k. This prevents the measured samples from overpowering the underlying low-quality samples for α close to many α_k. We set this value to one to ensure that the contribution of the histogram $h(\alpha|S_2)$ is at most equal to w_2. The weighted sum of the histograms for the ith bin can then be formulated as

$$h_i(\alpha, w_2|S_1, S_2) = h_i(\alpha|S_1) \cdot w_1(\alpha|S_2) + h_i(\alpha|S_2) \cdot w_2 \quad (6)$$

In the experiments presented in this paper, we define S_1 as the RCS samples produced through simulation and w_1 as the weight given to the histogram compiled from them, and correspondingly S_2 as the measured sparse RCS samples and w_2 as the weight given to the histogram compiled from them. In this paper, we will henceforth refer to the weight w_2 as w_m and the histogram produced using (6) as $h(w_m)$.

III. Experimental results

Next, we demonstrate the proposed approach to estimate the distribution of RCS using measured samples of a Volkswagen Golf vehicle. We consider the estimation based on the measured samples in combination with preliminary histograms compiled of simulated RCS. First, we describe the RCS data we use and the conduction of these experiments. Then, we present results to indicate the value of the proposed approach in terms of three measures relating to its performance: a distance measure to indicate the similarity between histograms, the absolute difference between likelihood values to indicate the performance in applications related to non-cooperative targets, and the relative difference between the estimates of

(a)

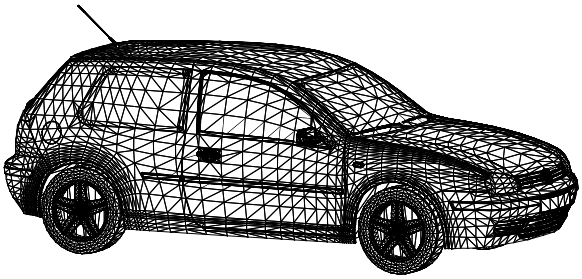

(b)

Fig. 1. The measured vehicle (a) and the 3D model used in the RCS simulation (b).

the maximum detectable range for a target to indicate the performance relating to radar performance prediction.

A. Description of the material

The data used in the experiments consist of measured and simulated RCS samples of a Volkswagen Golf vehicle. The measured samples have been collected at the frequency of 3 GHz on a turntable and cover the azimuth angles with a small step size and six elevation angles between 0° and 10°. For the purposes of this paper, we use the measured azimuth samples with a step size of one degree. Information on the measurement setup used in this paper has been described in more detail in [9]. The measured vehicle and the corresponding three-dimensional (3D) model (acquired from the Trimble 3D Warehouse) are shown in Fig. 1. The simulated RCS values have been computed using a method based on ray tracing and presented in [10] assuming the surface of the vehicle to be a perfect electric conductor (PEC).

Fig. 2 shows the measured and equivalently simulated RCS samples used in the experiments. As can be seen, the values differ in most aspect angles. Fig. 3 shows the RCS distributions estimated based on these samples for aspect angles α corresponding to the elevation angle of 5° and all azimuth angles with a one degree interval using (1) with $p(\alpha_k, \alpha) \sim N(\alpha, \sigma_1^2)$ and $\sigma_1 = 5^\circ$. The differences between the measured and simulated samples are mostly caused by the differences between the 3D model and the actually measured vehicle in regard to the shape of the surface as well as the material. As the simulated RCS has been produced assuming the vehicle to be a PEC, the material assumption for some of its parts—such as the wheels and the windows—is vastly incorrect. Then again, the use of a model not representing the true target accurately has its advantages: it offers us a baseline representation for the RCS with room for improvement, and thus allows us to demonstrate the benefits of the proposed approach.

B. Description of the experiments

In these experiments, we estimate the distribution of RCS with (6) using four different values for w_m while varying the sample size of the measurements. The values of w_m we consider are 0.00, 0.50, 0.75, and 1.0. We use $\sigma_1 = \sigma_2 = 5^\circ$, and thus the estimated distributions represent the selected aspect angles α, and the measured samples their estimated aspect angles α_k, with this uncertainty. Considering a practical application, the values of σ_1 and σ_2 should be chosen according to the circumstances, in the extreme case varying their values for each α and α_k.

The full measured data contain 2160 samples and we select eight different sample sizes from it: 1, 5, 10, 50, 100, 500, 1000, and 2160. We run a hundred repetitions in each case by randomizing the set of measured samples uniformly each time. We estimate the RCS distributions representing α at the elevation angle 5° and all the azimuth angles with a one degree interval in each case and repetition. As a comparison, we include a naive method that computes the histogram independent of the aspect angle using the available measured samples and denote it by h_{naive}. We consider the histogram produced from the full measurement data according to (1), shown in Fig. 3a, as the ground truth and denote it by h_{ref}. Fig. 4 shows the estimated RCS distributions of one repetition including h_{ref} for reference.

C. Performance analysis of the proposed approach

We analyze the performance of the proposed approach using the estimated RCS histograms, examples of which are shown in Fig. 4. We consider three measures of performance by comparing the ground truth and the estimated histograms: a histogram distance measure, the absolute difference of the likelihood value, and the relative difference of the estimated maximum detectable range.

We use the earth mover's distance (EMD) [11] to measure the distance between the estimated histograms and the ground truth. This choice of the distance measure is motivated by the intuitive interpretation of the distance value, which indicates the minimum cost needed to transform one histogram to another. The EMD also produces a sensible value for sparse histograms based on few samples, which conventional distance measures may not manage well. Let $emd(h_{ref}, h)$ represent the EMD between two histograms h_{ref} and h. We express the histogram distance as a percentage of the maximum cost $emd_{max}(h_{ref}, h)$ as

$$emd_{norm}(h_{ref}, h) = \frac{emd(h_{ref}, h)}{emd_{max}(h_{ref}, h)}. \quad (7)$$

The value of $emd_{max}(h_{ref}, h)$ represents the cost accrued by shifting all probability mass from one end of the histogram

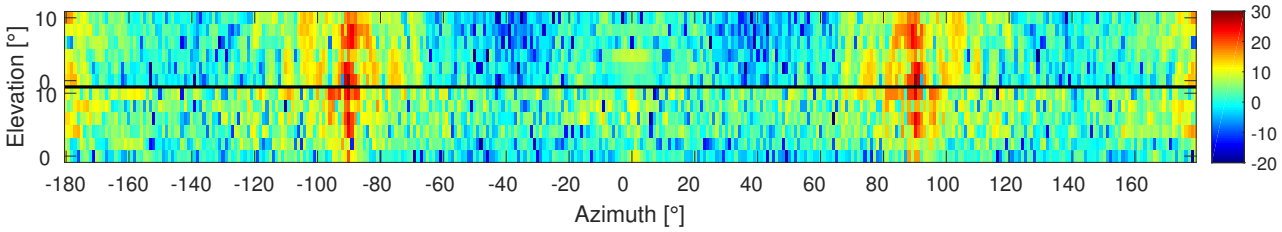

Fig. 2. The RCS of the Volkswagen Golf as dBsm in azimuth angles $-180°, -179°, ..., 179°$ and elevation angles $0°, 2°, ..., 10°$. The simulated values are presented at the top and measured values at the bottom. The azimuth angle $0°$ and elevation angle $0°$ correspond to viewing the target from the front. The azimuth angle increases towards the right side of the target and the elevation angle towards the top of the target.

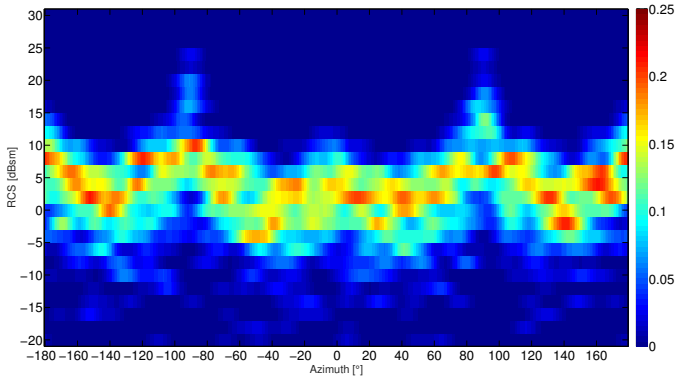

(a) Histograms compiled of the measured RCS samples.

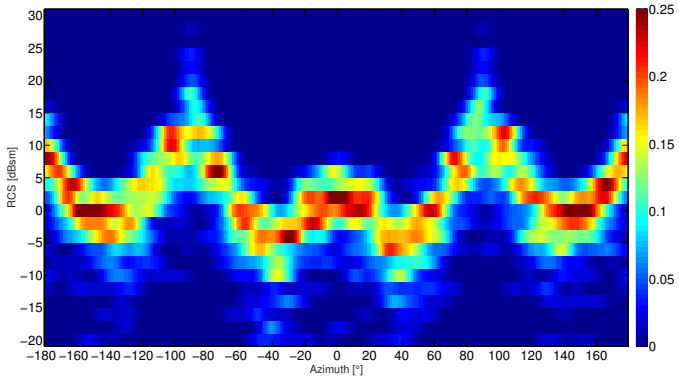

(b) Histograms compiled of the simulated RCS samples.

Fig. 3. Estimated RCS distributions according to (1) for the measured (a) and simulated (b) RCS samples shown in Fig. 2. The histograms have been produced at the elevation angle $5°$ and the azimuth angles with a one degree interval with the bin size of two dBsm and $\sigma_1 = 5°$. The vertical axis indicates the span of the histogram bins and the horizontal axis the aspect angle in azimuth.

to the other, and thus depends on the number of bins in the histogram. For instance, the shift of the probability mass in whole by one bin equals four percent in these experiments, where the histograms have 26 bins. Fig. 5 shows the results for the EMD with the different values of the w_m and the sample size. The results are presented averaged over the repetitions and the azimuth angles.

In order to produce an estimate for the performance in terms of the likelihood value for a specific aspect angle estimate, we need to determine how typical the RCS produced by its intended application is considering the estimated histogram. To simulate this process for the histogram h corresponding to the aspect angle α, we select one of the measured samples s_k randomly according to the distribution $p(\alpha_k, \alpha) \sim N(\alpha, \sigma_1^2)$ with $\sigma_1 = 5°$. The likelihood value is then determined for the RCS sample s_k from both the ground-truth histogram h_{ref} and the histogram h we compare it to. The likelihood of the measured sample $s_k \in \Delta_i$ is defined by

$$L(s_k, h) = h_i, \tag{8}$$

where h_i is the value of the ith histogram bin. Fig. 6 shows the results for the likelihood difference produced with the different values of the w_m and the sample size. The likelihood values are expressed as the absolute difference between the ground truth h_{ref} and the estimated histogram h

$$L_{diff}(s_k, h, h_{ref}) = |L(s_k, h) - L(s_k, h_{ref})|. \tag{9}$$

The difference values are presented averaged over the repetitions and the azimuth angles.

We consider the performance relating to radar performance prediction by analyzing the relative difference between the estimated maximum detectable range for a target. The error estimate of the maximum detectable range of a target is produced using a range coefficient

$$r(h) = \sum_i h_i \cdot \sqrt[4]{x_i}, \tag{10}$$

where x_i is the RCS at the center of the ith bin for histogram h expressed as square meters. We compute the range coefficient according to (10) for both the ground-truth histogram and the histogram we compare it with. The error estimate is the difference between the range coefficients expressed as a percentage value

$$e(h, h_{ref}) = \frac{|r(h_{ref}) - r(h)|}{r(h_{ref})}. \tag{11}$$

This relative difference between the range coefficients can be interpreted as the error in the estimation of the maximum range for an arbitrary radar system concerning the target in question. Fig. 7 shows the error of the maximum detectable range produced with the different values of the w_m and the sample size. The results are presented averaged over the repetitions and the azimuth angles.

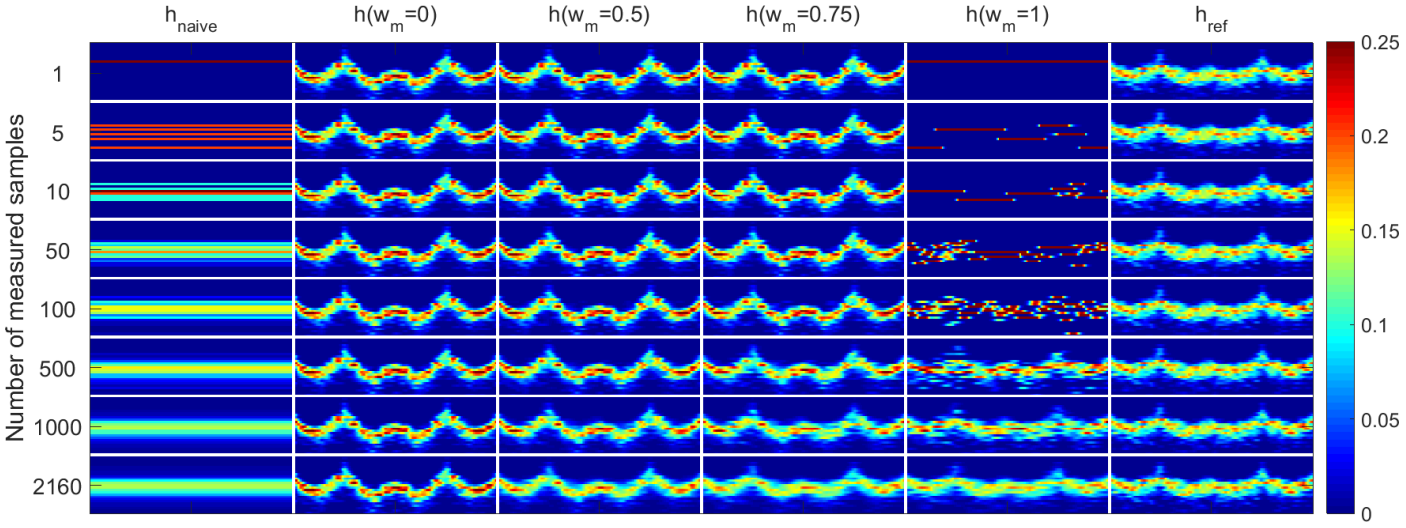

Fig. 4. The estimated RCS histograms for one repetition of the experiment. The histograms for each case correspond to elevation angle 5° and all azimuth angles with a one degree interval. The different sample sizes are presented on the vertical axis and different estimation methods on the horizontal axis separated by white lines. The presentation of each case corresponds to Fig. 3.

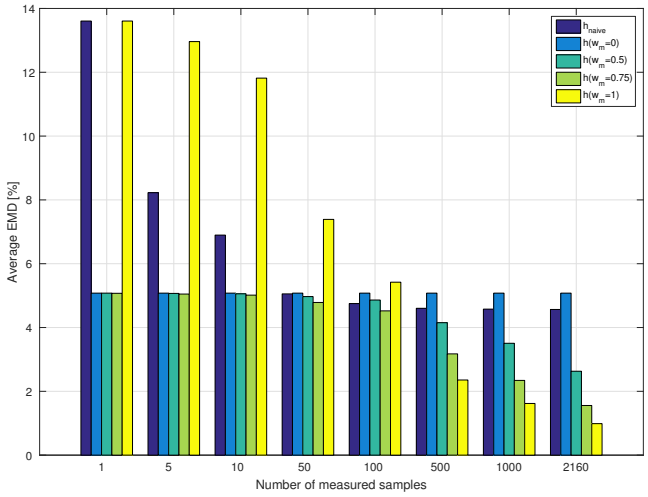

Fig. 5. The average EMD values for the different cases in the experiment. The results represent the elevation angle 5° with $\sigma_1 = 5^\circ$ and have been averaged over a hundred repetitions and the 360 different azimuth angles. The figure presents the average distance between the ground truth and the estimated distributions expressed as a percentage of the maximum value.

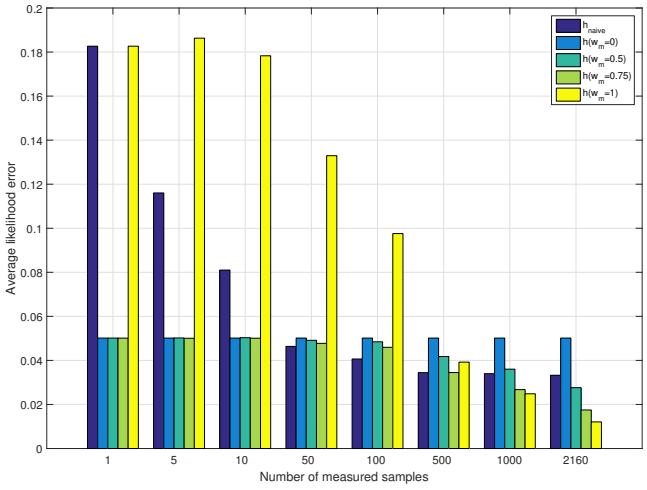

Fig. 6. The average likelihood error for the different cases in the experiment. The results represent the elevation angle 5° with $\sigma_1 = 5^\circ$ and have been averaged over a hundred repetitions and the 360 different azimuth angles. The figure shows the average absolute difference from the ground truth likelihood value for an aspect angle randomly selected according to $p(\alpha_k, \hat{\alpha})$.

IV. Discussion

In this paper, we proposed an approach to estimate the distribution of RCS using sparse measured samples. In the experiments, we considered a varying sample size and analyzed the performance of the method. As we can judge by the results presented in Fig. 4, Fig. 5, Fig. 6, and Fig. 7, the performance increases based on all three measures as the number of measured samples increases. The results also suggest that a small sample size benefits from relying more on the preliminary distribution (i.e. using a small value of w_m), whereas a large value of w_m is advantageous for a large sample size. The overall best performance seems to be achieved with a quite high value for w_m, in the order of 0.8–0.9. However, considering a practical system, the use of a high value of w_m may not be reasonable since the measured RCS may vary due to the operating conditions. The measured samples may also include a calibration error, which was not considered in these experiments. Moreover, the appropriate value for w_m is application-specific and should be determined based on a more extensive experiment than presented here considering multiple targets with multiple 3D models of different quality.

The experiments and analysis of this paper were conducted with a single test object. Consequently, the presented results should not be considered as an absolute truth but representing a case study. The test object in this paper was a car but any type of a target including aircraft and military targets could be

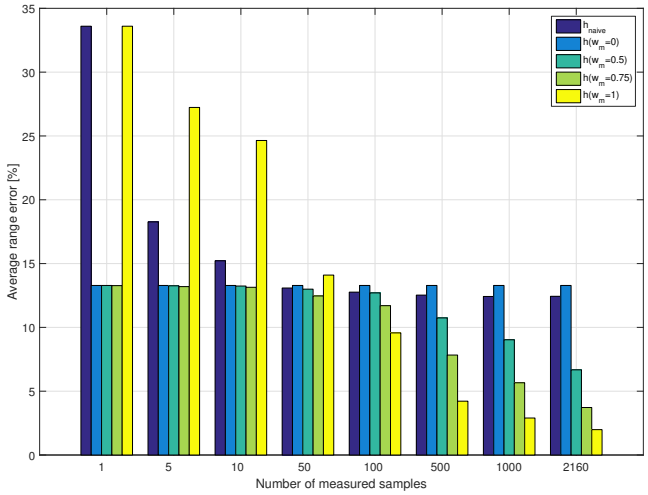

Fig. 7. The average error of the maximum detectable range for the different cases in the experiment. The results represent the elevation angle 5° with $\sigma_1 = 5^\circ$ and have been averaged over a hundred repetitions and the 360 different azimuth angles. The figure shows the average range error as a percentage of the ground-truth range coefficient.

considered with the proposed approach. As can be judged by Fig. 2, the 3D model used to compute the simulated RCS in these experiments corresponds only roughly to the measured vehicle.

We considered three measures of performance for the estimated RCS histograms: 1) a histogram distance measure, 2) the absolute difference of the likelihood value, and 3) the relative difference of the estimated maximum detectable range. Besides providing an assessment of the performance, these measures give an indication of the quality of the 3D model and the RCS simulation method. For instance, the similarity between simulated RCS and a measured sample set could be exploited in the selection of a suitable 3D model for a target. The quality of the simulation model used as the basis for the preliminary RCS estimate dictates the performance increase achievable with the proposed method: with a perfect simulation model there is no room for improvement, while a completely inaccurate model could be improved immensely. Furthermore, if no simulation model is available for the target or the target type is unknown, the proposed method can be used either without a preliminary estimate of the RCS (i.e. using $w_m = 1.0$) or with a more general type of simulation model, such as a generic car or an airplane with similar proportions.

In the presented results, we assume the histograms produced using (1) from all the measured data as the ground truth, whereas the different cases we compare it with are produced using (6). Since only the latter one of these equations includes the uncertainty about the aspect angle for the RCS samples, they do not produce the same result with the same data. Consequently, the comparison between these histograms is not entirely commensurable. In the experiments, we use the same data set to form the ground truth and the histograms we compare it with. To increase the validity of the comparison, the ground truth should preferably be compiled of other measurements representing diverse conditions. If this were the case, the performance of the proposed approach, when relying on the measured samples, would probably change from the assessments made here. However, our choice of the ground truth allows us control of the experiments since we can be certain the presented performance differences are due to the proposed approach and not due to the differences in the underlying data. The use of a more realistic ground truth is, thus, justifiably left as a subject for a more extensive experiment in the future.

V. Conclusion

The approach proposed in this paper allows the estimation of the distribution of RCS using a small number of measured samples. The estimation is further enhanced by applying the proposed concepts to refine a preliminary description of the target RCS of lower quality. The presented experiments demonstrate the approach and its benefits considering potential applications.

Acknowledgment

The research presented in this paper was conducted within the Finnish Defence Forces Research Program 2017. The authors would like to thank the Finnish Defence Forces and Patria Aviation for funding, support, and successful cooperation.

References

[1] A. De Maio, A. Farina, and G. Foglia, "Target fluctuation models and their application to radar performance prediction," *IEE Proceedings – Radar, Sonar and Navigation*, vol. 151, no. 5, p. 261–269, October 2004.

[2] R. D. Pierce, "RCS characterization using the alpha-stable distribution," *1996 IEEE National Radar Conference*, p. 154–159, 1996.

[3] D. Lewinski, "Nonstationary probabilistic target and clutter scattering models," *IEEE Transactions on Antennas and Propagation*, vol. 31, no. 3, p. 490–498, May 1983.

[4] W. Shi, X.-W. Shi, and L. Xu, "RCS characterization of stealth target using X2 distribution and lognormal distribution," *Progress In Electromagnetics Research M*, vol. 27, p. 1–10, 2012.

[5] B. Persson and M. Norsell, "Conservative RCS Models for tactical simulation," *IEEE Antennas and Propagation Magazine*, vol. 57, no. 1, p. 217–223, Feb 2015.

[6] M. Väilä, J. Jylhä, H. Perälä, and A. Visa, "Performance evaluation of radar NCTR using the target aspect and signature", *2014 IEEE Radar Conference*, p. 623–628, May 2014.

[7] M. Väilä, J. Jylhä, T. Sailaranta, H. Perälä, V. Väisänen, and A. Visa, "Incorporating a stochastic model of the target orientation into a momentary RCS distribution," *2015 IEEE Radar Conference (RadarCon)*, p.969–973, May 2015.

[8] M. Väilä, J. Jylhä, V. Väisänen, H. Perälä, A. Visa, M. Harju, and K. Virtanen, "A RCS model of complex targets for radar performance prediction," *2017 IEEE Radar Conference (RadarConf)*, p. 430-435, May 2017.

[9] H. Perälä, M. Väilä, J. Jylhä, J. Kylmälä, V.-J. Salminen, and A. Visa, "On efficient characterization of radar targets with scatterer sets for target recognition using commercial ray tracing software", *2014 IEEE Radar Conference*, 2014.

[10] H. Perälä, M. Väilä, and J. Jylhä, "M-SPURT—Compressing the target characterization for a fast monostatic RCS simulation," *International Conference on Radar 2018*, in press.

[11] Y. Rubner, C. Tomasi, and L. J. Guibas, "A metric for distributions with applications to image database," *Sixth International Conference on Computer Vision*, p. 59-66, 1998.